UDK 669.15-194.57:621.791.75
Original scientific article/Izvirni znanstveni članek

ISSN 1580-2949
MTAEC9, 57(3)241(2023)

# STUDY OF DROPLET TRANSFER CHARACTERISTICS AND WELD FORMATION WITH ER430LNb FERRITIC STAINLESS STEEL DURING GAS METAL ARC WELDING

## PREIZKUS LASTNOSTI PRENOSA KAPLJIC TALINE IN NASTAJANJA ZVARA FERITNEGA JEKLA VRSTE ER430LNB MED OBLOČNIM VARJENJEM V TOKU PLINSKE MEŠANICE KISIKA IN ARGONA

**Feng Liu[1], Yu Gu[2], Fanghong Xu[2], Han Zhang[1], Shaowei Xu[1], Zhihang Yan[1], Zhifeng Yan[1], Wenxian Wang[1]***

[1]College of Materials Science and Engineering, Taiyuan University of Technology, 79 West Yingze Street, Taiyuan 030024, Shanxi Province, China
[2]Shanxi Taigang Stainless Steel Co., Ltd., Taiyuan 030003, China

*Prejem rokopisa – received: 2022-11-26; sprejem za objavo – accepted for publication: 2023-03-16*

doi:10.17222/mit.2022.697

An ER430LNb ferritic stainless steel wire was used for a gas metal arc welding (GMAW) test. The characteristics of droplet transfer and its corresponding voltage and current waveforms were investigated using a high-speed camera and synchronous acquisition of electrical signals. The weld formation, droplet transfer patterns and corresponding microstructures under different welding parameters were observed, and the effect of the current level on the droplet transfer frequency was discussed. As the results show, there were three typical metal transfer patterns during the GMAW using the ER430LNb ferritic stainless steel wire, namely short circuit transfer, mix transfer and spray transfer. With an increase in the welding current, the weld formation is changing constantly, and the droplet transfer frequency increases exponentially. With the change in the transfer pattern, the columnar ferrite structure of the weld is continuously coarsening. In addition, hardness measurements were taken on joints welded at different welding currents for comparison.

Keywords: ER430LNb ferritic stainless steel wire, droplet transfer, weld formation, hardness

Za preizkuse obločnega varjenja v toku plinske mešanice kisika in argona (GMAW; angl:: gas metal arc welding) so uporabili žico iz nerjavnega feritnega jekla ER430LNb. S pomočjo uporabe sistema za opazovanje s hitro kamero in sinhronega zajemanja električnih signalov so raziskovali lastnosti prenosa kapljic taline ter odgovarjajoče napetostno in tokovno obliko valov. Med preizkusi so opazovali in nato obravnavali nastajanje zvara, vzorcev prenosa kapljic taline in nastanka odgovarjajoče mikrostrukture pri različnih izbranih parametrih varjenja. Rezultati preizkusov in opazovanj so pokazali, da potekajo trije tipični vzorci prenosa kapljic taline pri GMAW z uporabo žice iz nerjavnega feritnega jekla ER430LNb in sicer: kratko stični prenos, mešani prenos in prenos v obliki razpršila. Z naraščajočim varilnim tokom se nastajanje zvara konstantno spreminja in frekvenca prenosa kapljic taline narašča eksponentno. S spremembo vzorca prenosa taline stebričasta feritna struktura zvara kontinuirno postaja bolj groba. Dodatno so s pomočjo meritev trdote zvarnih spojev medsebojno primerjali njihove lastnosti glede na izbrane parametre varjenja.

Ključne besede: varilna žica iz feritnega jekla vrste ER430LNb, prenos kapljic taline, nastajanje zvara, trdota

## 1 INTRODUCTION

Ferritic stainless steels are widely used in various areas, including automobile manufacturing, white goods and nuclear power industries, as they exhibit a good combination of ductility, thermal conductivity and corrosion resistance. Their cost is also relatively lower and more stable than those of austenitic grades as they do not contain any nickel.[1–3] As a relatively new type of engineering material, ER430LNb ferritic stainless steel with excellent comprehensive properties is produced by partially or completely replacing nickel with niobium to reduce the alloying-element costs. Deardo et al.[4] pointed out that the precipitation of NbC, NbN, $Fe_2Nb$ and other intermetallic compounds formed in steel by Nb, a strong carbide-forming element, significantly improved the mechanical properties of ER430LNb at high temperatures,[5,6] effectively prevented the intergranular chromium poverty caused by the precipitation of carbon-chromium compounds, and improved the resistance to intergranular corrosion.[7]

Different forms of droplet transfer have various consequences for the stability of the welding arc, the depth of fusion of the weld, spatter and the generation of defects and they affect the quality of the weld-seam formation. Oscillography and high-speed camera technology are two of the main experimental tools used for studying droplet transfers.[8] Oscillography records the waveform of the welding current and arc voltage during a welding process and indirectly researches the droplet transfer based on the waveform modification. A high-speed cam-

*Corresponding author's e-mail:
wangwenxian@tyut.edu.cn (Wenxian Wang)

era captures the welding arc zone with a high-speed video; a droplet-transfer process is recorded, and through an analysis of droplet transfer images we directly investigate the characteristics of the droplet transfer. The combination of oscillography and a high-speed camera allows us to better investigate the characteristics of a droplet transfer. The droplet transfer of GMAW has been extensively studied by domestic and international scholars. Luo et al.[9] discussed the relationship between the droplet-transfer behavior and arc current-voltage signal and found that the characteristics of the droplet-transfer behavior depend on the arc current-voltage signal. Neyka et al.[10] investigated the droplet-transfer behavior of Tandam based on the high-speed camera technology. Simpson et al.[11] showed theoretically that when the welding current is less than 250 A, the shape of the droplet is approximately spherical. Praveen et al.[12] combined a high-speed camera and oscillography to research droplet-transfer patterns during a pulsed-welding process. Hu and Tsai et al.[13] investigated the droplet-transfer behavior at constant and pulsed currents through numerical simulations, indicating that the higher the welding current, the greater is the electromagnetic force on the droplet and the easier is the droplet transfer from the wire to the base material. It was also found that the higher the welding current, the smaller is the droplet diameter and the higher is the droplet transfer frequency.

Therefore, this work investigates the droplet transfer characteristics and weld formation of stainless steel in an GMAW process. The droplet transfer frequency, microstructure and hardness of joints welded at different welding currents were studied for comparison. The results of the study lay the foundation for the subsequent process optimization of the gas-shielded welding of ER430LNb ferritic stainless steel.

## 2 EXPERIMENTAL PROCEDURE

The experimental system for the research of the GMAW using an ER430LNb ferritic stainless steel wire is shown in **Figure 1**; it mainly includes a robotic GMAW system and a synchronous acquisition of droplet transfer and electrical parameters. The robotic GMAW system includes a welding robot and its control cabinet, welding power supply, gas supply system and working platform to provide a stable droplet-transfer process. The electrical-signal synchronous acquisition system includes a high-speed camera, xenon light source and Hanover analyzer to capture the images and electrical signals of the droplet-transfer process in real time. A 6-axis OTC AX-V6 welding robot and YD-500GL3 welding power source are utilized to sustain stable arc burning. A MIX-L25 gas-mixture cabinet adjusts the content of argon and oxygen. The CR3000×2 high-speed camera operating at 3000 fps in the same line as the 1000 W xenon lamp light source generator and the welding torch remain relatively stationary. The AH19 Hanover analyzer acquires the data from the characteristic signals of voltage and current during the welding process.

The base material (BM) included 4.0 mm thick plates of AISI 430 ferritic stainless sheets and the welding wire was an ER430LNb ferritic stainless steel wire with a diameter of $\phi$1.2 mm. **Table 1** lists the main components of the welding wire and the base metal. Meanwhile, the welding parameters are listed in **Table 2**. The welding current was the crucial research variable in this work. The welding speed was selected in a range of 10–100 cm/min. The wire feed speed (WFS) was automatically matched with the GMAW power supply according to the welding current. But the welding current and arc voltage can be adjusted independently. To simplify the experiment, the droplet transfer was captured

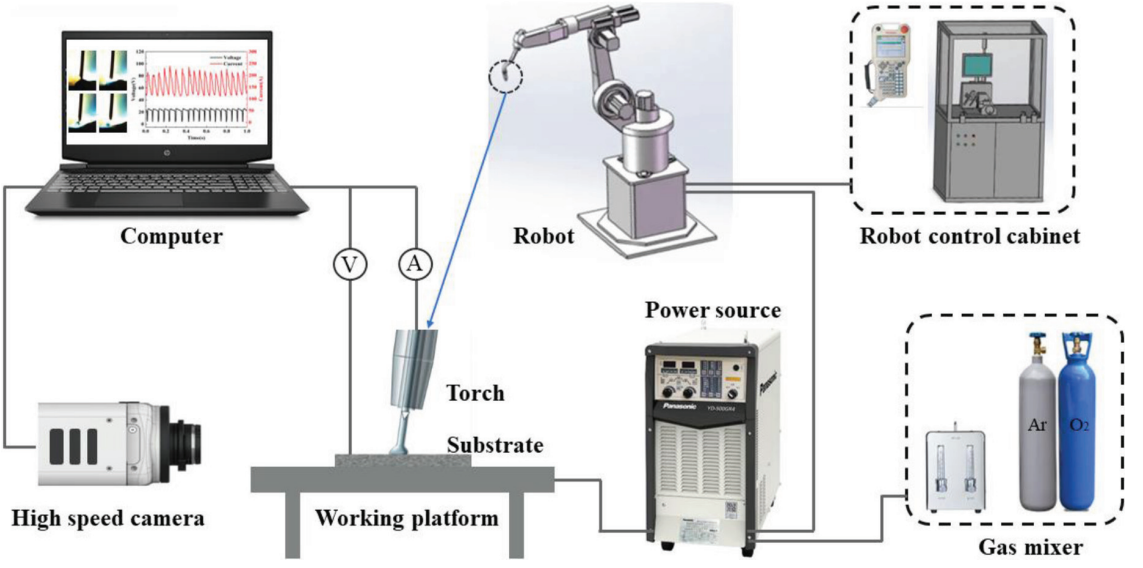


**Figure 1:** Schematic diagram of the experimental system

**Table 1:** Main components of the welding wire and the base metal (*w*/%)

| Element | C | Si | Mn | P | S | Cr | Ni | Mo | N | Cu | Nb | Fe |
|---|---|---|---|---|---|---|---|---|---|---|---|---|
| Welding wire | 0.03 | 0.5 | 0.6 | 0.03 | 0.03 | 15.5–17.0 | 0.6 | 0.75 | – | 0.75 | 0.24–1.2 | Balance |
| Base metal | 0.10 | 0.5 | 0.6 | 0.03 | 0.02 | 15.5–17.0 | 0.6 | 0.75 | – | 0.75 | – | Balance |

**Table 2:** Various welding parameters

| | 1 | 2 | 3 | 4 | 5 | 6 | 7 | 8 | 9 | 10 |
|---|---|---|---|---|---|---|---|---|---|---|
| Welding speed (cm/min) | 40 | | | | | | | | | |
| Welding current (A) | 60 | 78 | 90 | 110 | 120 | 138 | 162 | 178 | 198 | 214 |
| Arc voltage (V) | 17.6 | 18 | 18.8 | 20.4 | 20.6 | 21.6 | 22.4 | 23.6 | 25.6 | 27 |

using the method of overlay welding on the plate workpiece.

For the post-weld analysis, samples were cut using wire electro-discharge machining. For the optical-microscope testing, the sample was polished using emery paper with grit sizes of 600, 1000, 1500 and 2000. Finally, cloth polishing was done using 1-μm diamond paste to achieve a mirror finish of the weld cross-section. After polishing, the weld interface was etched with a Marble reactant etching solution (4 g $CuSO_4$ + 20 mL HCl + 100 mL $H_2O$) and the microstructure was observed with an optical microscope (BH200M). The crystal structure was characterized, using an X-ray diffractometer (XRD, D/MAX-2400) with Cu $K_\alpha$ radiation. The scanning range was from 30° to 100° in $2\theta$ at a scanning rate of 5°/min. A nanoindentation test (Nano indenter G200) was used to measure the hardness of welded joints, with a load of 80 mN.

## 3 RESULTS AND DISCUSSION

### *3.1 Three typical metal transfer patterns*

There were three typical metal transfer patterns observed during the GMAW using the ER430LNb ferritic stainless steel wire, namely the short circuit transfer, mix transfer and spray transfer.

Short circuit transfer

A droplet is short-circuited to the welding pool at low current and voltage before completing its growth. Under the effects of surface tension, gravity and electromagnetic forces, the droplet transfers to the base material, forming a short-circuit transfer.

During the short-circuit transfer, a lot of spatter is observed (**Figure 2e**) as the arc voltage increases with the increasing welding current. In general, at low wire feed speeds, the droplet-transfer pattern in a GMAW process is either a short-circuit transfer or a particle transfer, depending on the arc voltage. **Figure 2** shows the curves of the electrical parameter signals during the ER430LNb GMAW process within 1 s and the complete transfer of a droplet from wire tip generation, growth and then transfer into the welding pool. The I and U in the figures illustrate the average welding current and average arc voltage. When the welding current is moderate, the short circuit transfer can be found to include three stages of short circuit, arc reignition, and droplet growth. The wire feed speed and welding current are relevant, and, as can be found in **Figure 2**, when the welding current increases, the wire feed speed increases as well, while the transfer period and arc initiation time for a single droplet gradually decrease.

The droplet size affects the magnitude of gravity, arc force, etc. during the droplet-transfer process, resulting in different impacts of the liquid melt pool, thus affecting the melt pool flow forming. The change in the droplet size during the droplet transfer from **Figure 2d** is shown in **Figure 2g**. From $t_0$ s to $t_0$ + 0.152 s, the droplet diameter and size are marked in the voltage-waveform figure with the time variation. The droplet diameter is 2.0 mm at $t_0$ + 0.032 s. It increases to 2.3 mm and 2.6 mm after 0.33 s and 0.73 s, respectively, and reaches a maximum of 2.7 mm at $t_0$ + 0.141 s. The droplet size decreases after $t_0$ + 0.148 s to a diameter of 2.6 mm, which rapidly decreases to 2.0 mm after 0.04 s.

During several droplet transfers within 1 s on the graph, the welding current and arc voltage patterns remain largely unchanged, indicating a relatively stable welding process. The wire tip returns to 1.2 mm after 0.03 s and the melt droplet transfer process ends. In summary, the short-circuit transfer is stable at a low wire feed speed and a suitable welding current. **Figures 2** to **4** show that the electrical voltage signal does not go to zero at the time of the short circuit. Additionally, to smoothen the wave, the collected data of electrical signals are processed by mean filtering. The measured short circuit voltage increases after mean filtering, and it is not equal to zero when the short circuit occurs. As the proportion of short circuit transients is very small, it has little influence on the analysis of electrical parameters.

#### *3.1.1 Mix transfer*

The welding current of mix transfer is between those of short circuit transfer and spray transfer. The metal transfer patterns include both particle transfer and short circuit transfer, but the proportions vary randomly. With the increase in the welding current, the arc current-voltage signal becomes more disordered between the short circuit transfer from **Figure 3a** and the mix transfer from **Figure 3b**, with both short-circuit and particle transfer. The welding current continues to increase and the drop-

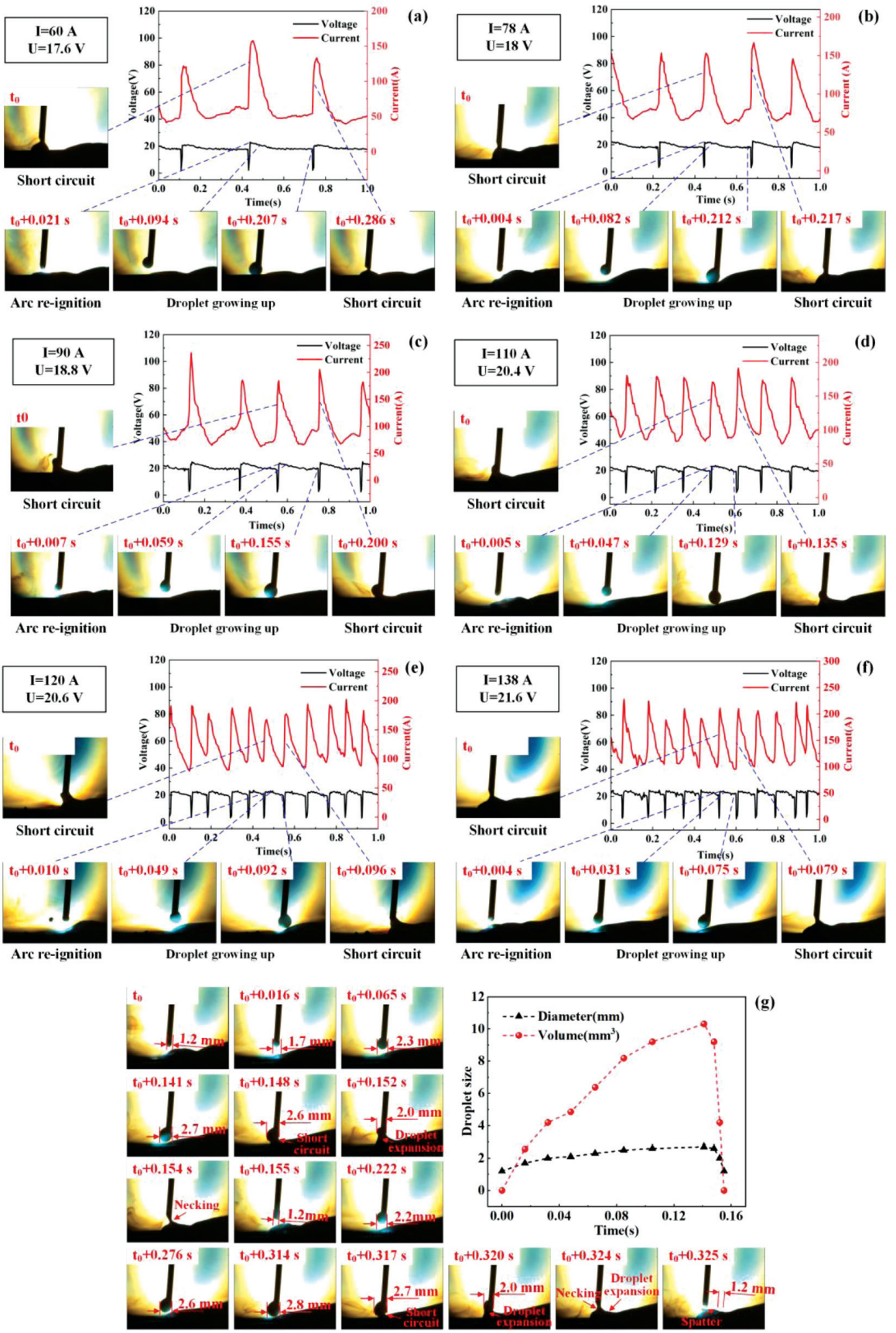


**Figure 2:** Droplet transfer and electric signals: a) I = 60 A, b) I = 78 A, c) I = 90 A, d) I = 110 A, e) I = 120 A, f) I = 138 A, g) change in droplet size at 110 A

let for the complete particle transfer pattern is shown in **Figure 3c**. The molten droplet size decreases close to the wire diameter, and the molten droplet transfer occurs along the wire axis. The welding current continues to increase, and we see a fully particle-transfer pattern in **Figure 3c**, with droplets falling along the axis of the wire. In addition, the droplet size decreases close to the wire diameter.

Compared to the short circuit transfer, it can be seen from the voltage-current signal diagram that the frequency of the mix transfer increases significantly. **Figure 3c** shows that the frequency of the particle transfer is very fast, and the actual number of transfers per second can reach 50. However, the reason why the periodic frequency of the electric signal is only 4–5 is that the instability of the particle transfer causes a periodic short circuit. As the welding current increases to 198 A, the droplet-transfer pattern changes from short circuit and particle transfer to a completely particle transfer.

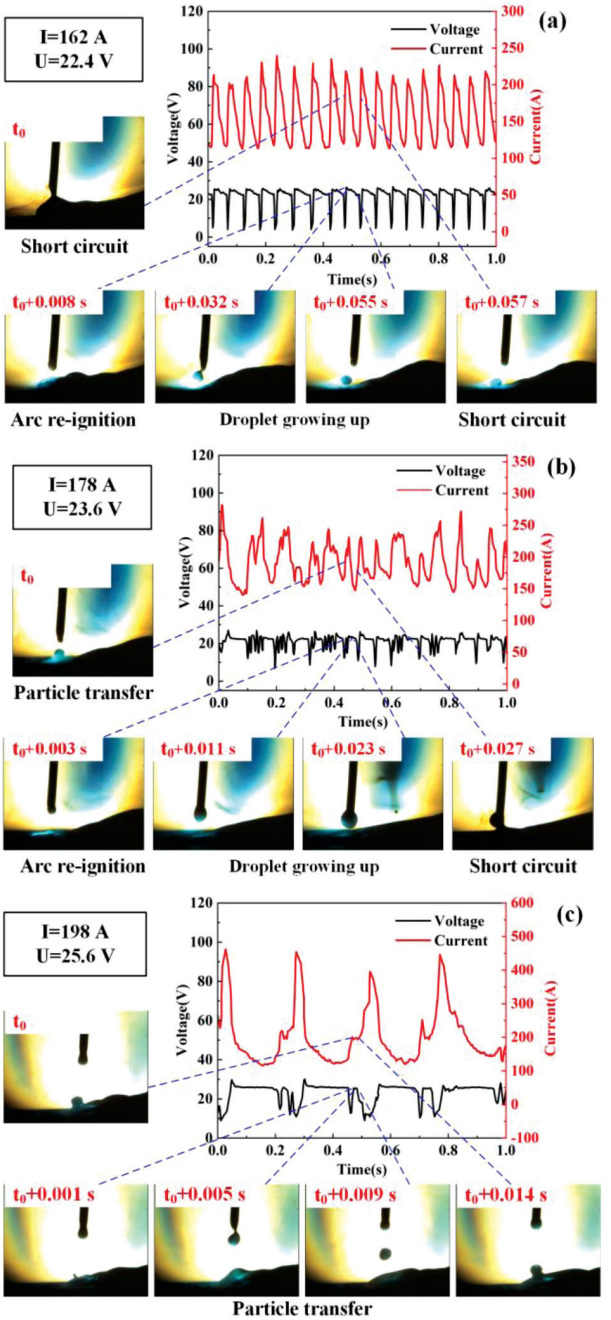


**Figure 3:** Droplet transfer and electric signals: a) I = 162 A, b) I = 178 A, c) I = 198 A

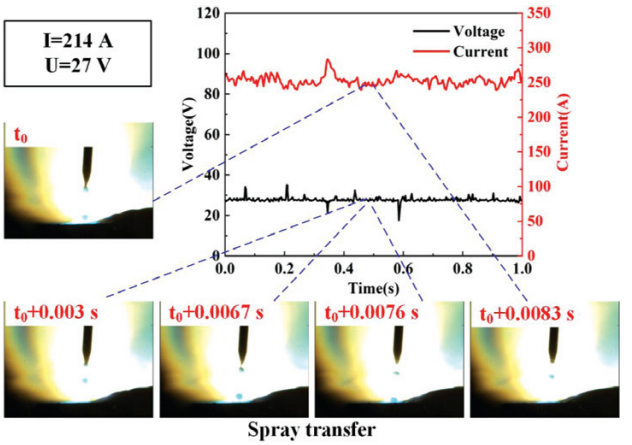


**Figure 4:** Droplet transfer and electric signals at 214 A

### *3.1.2 Spray transfer*

As shown in **Figure 4**, when the welding current increases to 214 A, the droplet-transfer pattern changes from mix transfer to spray transfer. During the process of spray transfer, a droplet with a diameter smaller than that of the welding wire is generated from the tip of the welding wire and it falls off. Before the previous droplet falls into the molten pool, the next droplet has been generated, starting to fall off. The transfer frequency of droplets is very high, and the number of transfers per second can reach hundreds of times.

## *3.2 Weld formation*

The weld formation at different GMAW parameters is shown in **Figure 5**. For a stable short circuit transfer, a good weld surface is demonstrated in **Figure** 5, with negligible welding spatter where the welding process is relatively stable. When the current increases to 162 A, the droplet impacts the surface of the liquid molten pool at the same time as the short circuit transfer so that the droplet transfer is unstable and the splash is large. When the welding current increases to 210 A or more, the width of the weld increases sharply, and the weld surface is badly formed, generating a lot of spatter and fumes. Different welding currents used for the weld formation are indicated in **Figure 5d**. It is worth mentioning that under each welding process parameter, the residual height of the weld does not change significantly.

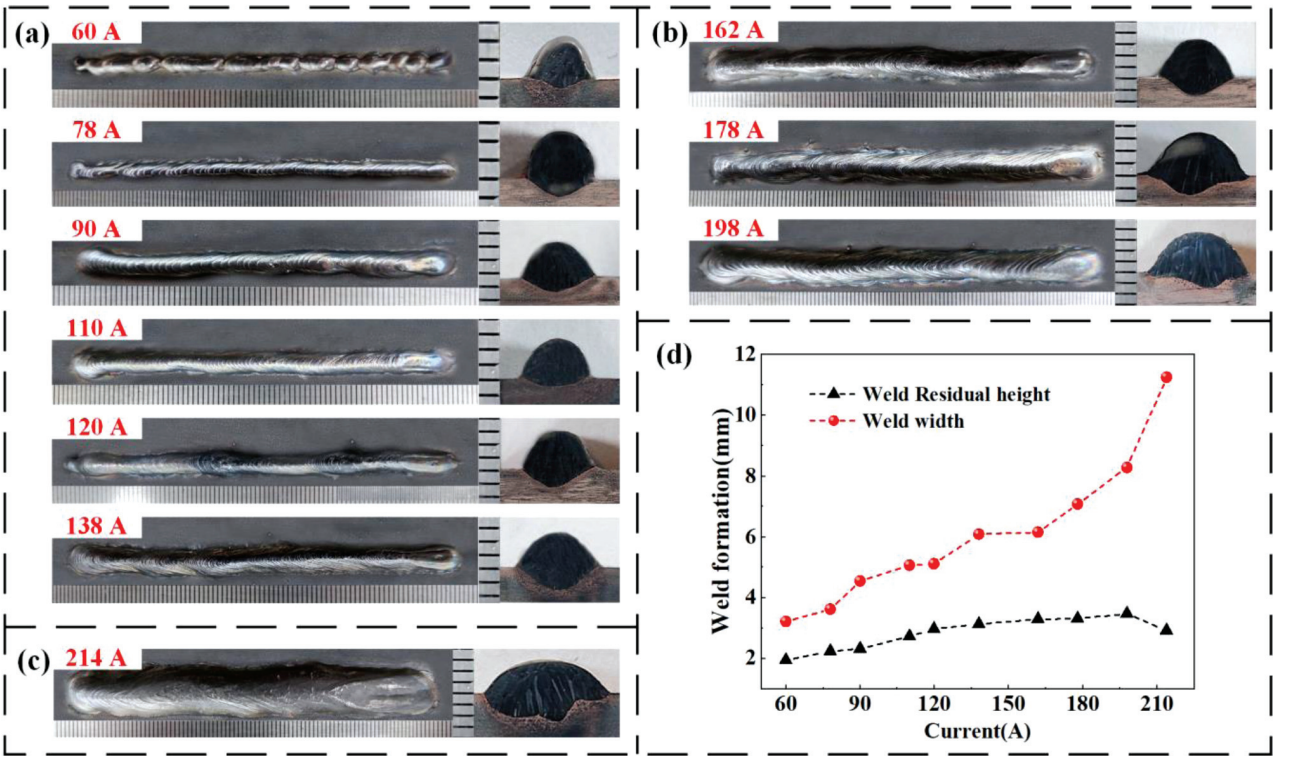


**Figure 5:** Weld formation: a) short circuit transfer, b) mix transfer, c) spray transfer, d) weld formation at different welding currents

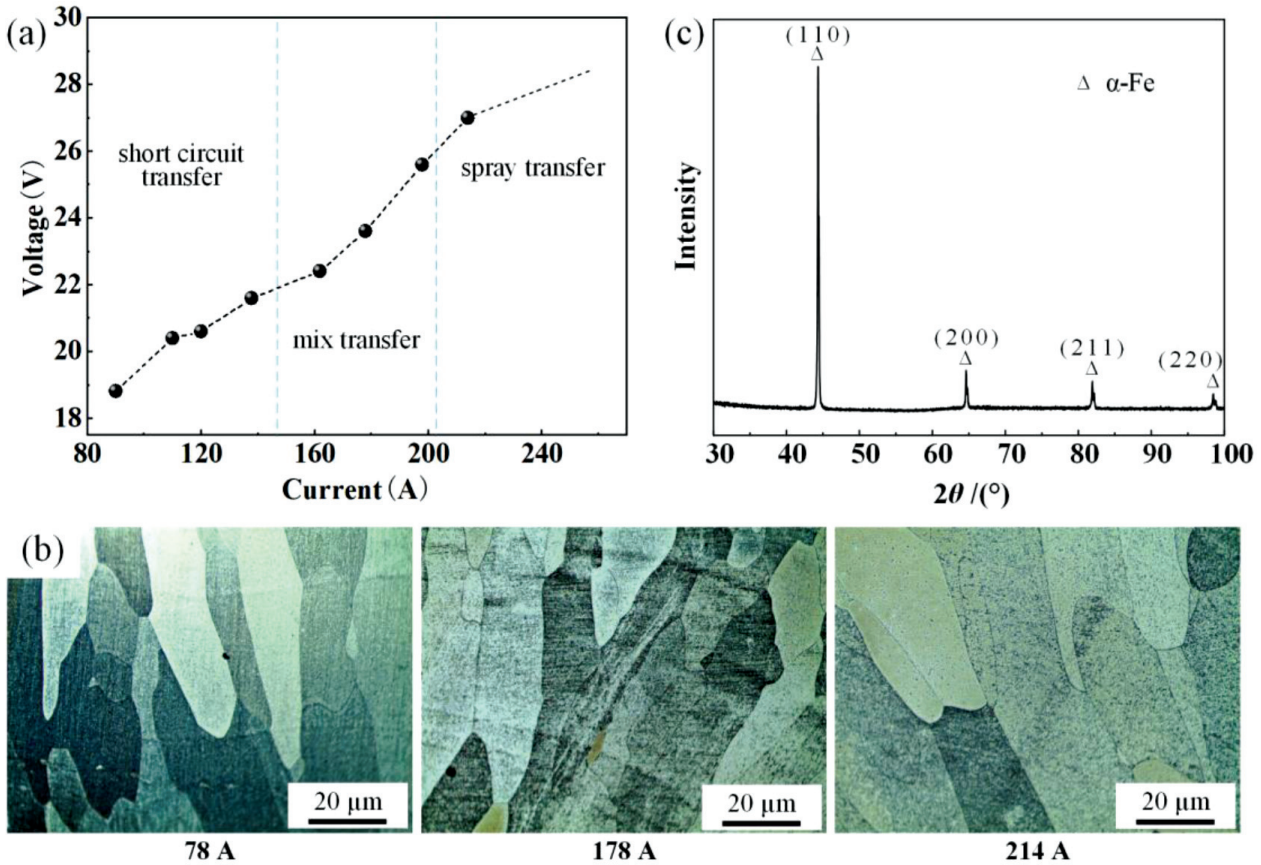


**Figure 6:** Droplet transfer patterns and microstructure: a) droplet transfer patterns, b) microstructure for different droplet transfer patterns, c) XRD pattern of weld joints

### *3.3 Droplet transfer patterns, microstructure and droplet transfer frequency*

With an increase in the welding parameters, the droplet transfer pattern changes gradually. As shown in **Figure 6a**, the droplet transfer pattern can be divided into three kinds: the short circuit transfer with small parameters, the mix transfer and the spray transfer. A set of parameters, including 78 A, 178 A and 214 A, for each transfer pattern was selected to observe the microstructure. It can be seen that the microstructure is coarse columnar ferrite, and the ferrite grain is also continuously coarse with the increasing welding current, as shown in **Figure 6b**. According to the XRD results shown in **Figure 6c**, the phase composition of the weld is a 100 % ferrite structure.

The droplet transfer frequency is a very important parameter, closely related to the welding efficiency and weld formation. A higher droplet transfer frequency causes a higher welding efficiency. With the increasing welding parameters, the droplet transfer frequency also changes gradually. For a weld formed of ferritic stainless steel, a small welding current with a moderate droplet transfer frequency is preferred. The droplet transfer frequency increases exponentially as shown in **Figure 7**. The regression fitting of the welding current to the droplet transfer frequency was obtained using the Origin software, and the equation is as follows:

(3-1)

### *3.4 Hardness test*

Five welding parameters were selected for hardness testing of three different droplet transfer patterns by a nanoindentation test. **Figure 8** shows typical microhardness distributions with different welding currents for the three main welding zones: the base metal, HAZ and weld metal. A variation caused by nanoindentation was observed in the microhardness values from the base material to the weld metal.

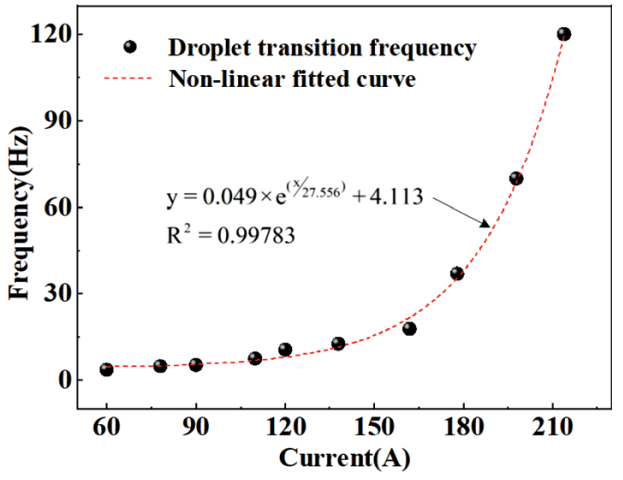


**Figure 7:** Non-linear fitted curves of droplet transfer frequency

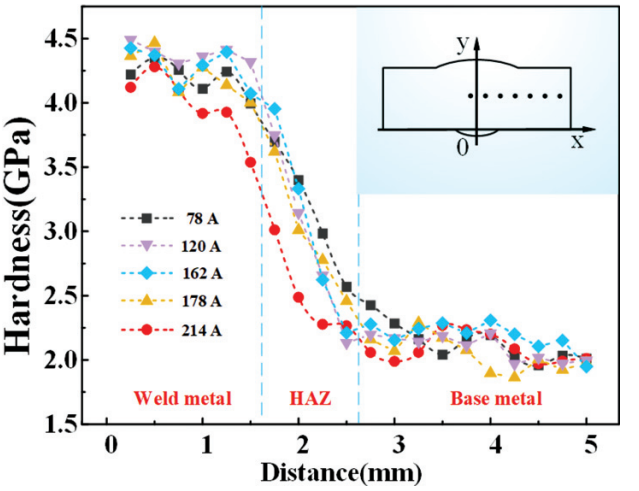


**Figure 8:** Hardness measurement results

The highest hardness values were measured on the weld metal, between 3.5 GPa and 4.5 GPa. The hardness values of the HAZ were found to be between 2.2 GPa and 3.9 GPa. It should be underlined that the base metal has softer regions (1.8–2.3 GPa) than the HAZ. The increase in the hardness of the weld metal and base metal may be attributed to the changes in the microstructure through a relatively higher cooling rate due to the higher heat input during welding.

The overall hardness of the welding zone (HAZ and weld metal) decreased due to the increase in the welding current. With the increasing welding current, a higher heat input is generated during welding. Therefore, the cooling takes place at a higher temperature. Thus, the changes in the volume ratio of the phases formed in the microstructure may cause an increase in the hardness.

## 4 CONCLUSIONS

In this study, ER430LNb ferritic stainless steel used for gas metal arc welding was studied. The test results are summarized as follows:

(1) During the GMAW using an ER430LNb ferritic stainless steel wire, the droplet transfer is a stable short circuit transfer at currents of less than 138 A. The droplet transfer pattern is a mixed transfer at currents of around 162–198 A. And it is a spray transfer when the current is over approximately 214 A.

(2) During the short circuit transfer stage, the droplet size is approximately 2–3 times the diameter of the welding wire. With an increase in the current, the droplet transfer gradually changes to particle transfer, and the droplet size decreases gradually. As the current increases further, the droplet transfer pattern is spray transfer, and the droplet size is smaller than the diameter of the welding wire.

(3) With the increase in the welding current, the current-voltage signal becomes more disordered, resulting

in more welding splash and fumes. For gas metal arc welding with ER430LNb ferritic stainless steel, a low welding current with a moderate droplet transfer frequency is preferred.

(4) The weld microstructure of ER430LNb ferritic stainless steel indicates coarse columnar ferrite, and the grain size increases with the increase in the welding current. In addition, with a continuous increase in the welding current, the droplet transfer frequency increases rapidly and exponentially.

(5) The hardness distribution values for the weld joints of the weld metal, HAZ and base metal are 3.5–4.5 GPa, 2.2–3.9 GPa and 1.8–2.3 GPa, respectively. The hardness in the welding zone (HAZ and weld metal) decreases due to the welding current increase.

## Compliance with Ethical Standards

Funding: This study was funded by the National Natural Science Foundation of China (grant numbers 52274390 and 52075360).

## Conflicts of Interest

The authors declare that they have no conflict of interest.

## 5 REFERENCES

[1] K. A. Cashell, N. R. Baddoo, Ferritic stainless steels in structural applications, Thin-Walled Structures, 83 (2014)

[2] Y. Zhang, J. Guo, Y. Li, Z. Luo, X. Zhang, A comparative study between the mechanical and microstructural properties of resistance spot welding joints among ferritic AISI 430 and austenitic AISI 304 stainless steel, Journal of Materials Research and Technology, 9 (**2020**) 1

[3] Hao Fu, Jiawei Min, Hongshan Zhao, Yulai Xu, Pengfei Hu, Jianchao Peng, Han Dong, Improved mechanical properties of aluminum modified ultra-pure 429 ferritic stainless steels after welding, Materials Science and Engineering: A, 749 (2019)

[4] A. J. Deardo, Niobium in modern steels, International Materials Reviews, (**2013**), 371–402

[5] G. M. Sim, J. C. Ahn, S. C. Hong, K. J. Lee, K. S. Lee, Effect of Nb precipitate coarsening on the high temperature strength in Nb containing ferritic stainless steels, Materials Science and Engineering: A, 396 (**2005**) 1–2, 159–165

[6] N. Fujita, K. Ohmura, A. Yamamoto, Changes of microstructures and high temperature properties during high temperature service of Niobium added ferritic stainless steels, Materials Science and Engineering: A, 351 (**2003**) 1–2, 272–281

[7] W. Gordon, A. V. Bennekom, Review of stabilisation of ferritic stainless steels, Materials Science and Technology, 12 (**1996**) 2, 126–131

[8] Y. Bao, Y. Zhou, Y. Wu, Y. Wu, H. Yao, Study on metal transfer of MIG/MAG, Electric Welding Machine, 36 (**2006**) 3, 55–58

[9] Y. Luo, J. Li, J. Xu, L. Zhu, J. Han, C. Zhang, Influence of pulsed arc on the metal droplet deposited by projected transfer mode in wire-arc additive manufacturing, Journal of Materials Processing Technology, 259 (**2018**), 353–360

[10] S. Neyka, M. Kusch, P. Mayr, Progress in high performance hardfacing processes Tandem-Gas-Metal-Arc-Welding and Plasma-MIG Hybrid welding, (2013)

[11] S. W. Simpson, P. Zhu, Formation of molten droplets at a consumable anode in an electric welding arc, Journal of Physics D: Applied Physics, 28 (1**9**95) 8, 1594

[12] P. Praveen, M. J. Kang, P. Yarlagadda, Arc voltage behavior in GMAW-P under different drop transfer modes, Journal of Achievements of Materials and Manufacturing Engineering, 32 (**2009**) 2

[13] J. Hu, H. L. Tsai, Effects of current on droplet generation and arc plasma in gas metal arc welding, Journal of Applied Physics, 100 (**2006**) 5